Cracking in hydrogen ion-implanted $Si / Si_{0.8}Ge_{0.2} / Si$ heterostructures

Lin Shao, Y. Q. Wang, J. G. Swadener, M. Nastasi, Phillip E. Thompson, and N. David Theodore

Citation: Appl. Phys. Lett. **92**, 061904 (2008); doi: 10.1063/1.2838338
View online: https://doi.org/10.1063/1.2838338
View Table of Contents: http://aip.scitation.org/toc/apl/92/6
Published by the American Institute of Physics

Sensors, Controllers, Monitors
from the world leader in cryogenic thermometry

Cracking in hydrogen ion-implanted $Si/Si_{0.8}Ge_{0.2}/Si$ heterostructures

Lin Shao,[1,2,a)] Y. Q. Wang,[2] J. G. Swadener,[2] M. Nastasi,[2] Phillip E. Thompson,[3] and N. David Theodore[4]

[1]*Department of Nuclear Engineering, Texas A&M University, College Station, Texas 77843, USA*
[2]*Los Alamos National Laboratory, Los Alamos, New Mexico 87545, USA*
[3]*Code 6812, Naval Research Laboratory, Washington, DC 20375-5347, USA*
[4]*Analog and Mixed-Signal Technologies, Freescale Semiconductor, Inc., Tempe, Arizona 85284, USA*

(Received 14 November 2007; accepted 7 January 2008; published online 12 February 2008)

We demonstrate that a controllable cracking can be realized in Si with a buried strain layer when hydrogen is introduced using traditional H-ion implantation techniques. However, H stimulated cracking is dependent on H projected ranges; cracking occurs along a $Si_{0.8}Ge_{0.2}$ strain layer only if the H projected range is shallower than the depth of the strained layer. The absence of cracking for H ranges deeper than the strain layer is attributed to ion-irradiation induced strain relaxation, which is confirmed by Rutherford-backscattering-spectrometry channeling angular scans. The study reveals the importance of strain in initializing continuous cracking with extremely low H concentrations. © *2008 American Institute of Physics*. [DOI: 10.1063/1.2838338]

Driven by the need to provide ever higher density chips with higher speed and lower power consumption, silicon-on-insulator (SOI) wafers have become the substrates of choice for the fabrication of various microelectronic devices.[1] SOI wafers produced by the so-called "smart cut" technique[2] are synthesized by hydrogen ion implantation into silicon. Upon annealing, implanted hydrogen forms bubbles that provide the crack-opening displacements that drive long range cracking in a direction parallel to the surface. Using wafer bonding, the Si layer is transferred onto another surface-oxidized wafer to form a SOI structure, with the thickness of the transferred Si layer being roughly equal to the projected range of the H ions. However, H-ion implantation alone is not capable of producing ultrathin layer transfers. When ion energies are decreased to reduce the thickness of the transferred layer, the implantation damage begins to extend to the surface rendering the transfer layer unfit as an electronic material. During the past several years, innovations have been developed by our group which have shown that hydrogen induced exfoliation is now possible without the need of ion implantation.[3–6]

In our previous studies, we have demonstrated smooth cracking in Si at a depth less than 20 nm.[6] Such thin layer exfoliation is accomplished using a buried strained layer to trap H that is introduced via a hydrogen plasma. Under such conditions, H ions are accelerated toward the Si surface at very low energies (a few hundred eV) upon which they diffuse to and are trapped at the strained layer. Upon accumulation at the strained layer (100) hydrogen platelets and ultimately hydrogen bubbles are formed,[6] leading to controlled cracking along the strained-layer/Si interface. Given the potential of strained layers in Si to trap hydrogen and to produce cracking, we have carried out an investigation to study the role of the hydrogen energy on the exfoliation process. This was accomplished using H-ion implantation, where H ions were implanted to ranges less than or greater than the depth of the buried strained layer.

Strained layer samples were synthesized using molecular beam epitaxial (MBE) growth to fabricate a $Si/Si_{0.8}Ge_{0.2}/Si$ heterostructure. A 5-nm-thick $Si_{0.8}Ge_{0.2}$ layer was grown on a (100) Si substrate, followed by growth of a 200-nm-thick monocrystalline-Si capping layer. The samples were subsequently implanted with H ions at energies of 7 or 33 keV, with a dose of $5\times10^{16}/cm^2$. The substrates were heated at 300 °C during ion implantation to simulate hydrogenation conditions. As a comparative study, Czochralski-grown 15–20 Ω cm *p*-type (100) Si was also implanted under the same conditions. Depth profiles of H and Ge atoms were measured using secondary ion mass spectrometry (SIMS) by using 1 keV Cs^+ beams. Transmission electron microscopy (TEM) was used to characterize the sample structure. Channeling Rutherford-backscattering spectrometry (RBS) was used to measure strain by using the angular-scan technique. RBS was performed by using 2 MeV He^+ ions with a surface barrier detector located at 167° away from the beam-incident direction.

Figure 1 shows SIMS hydrogen and germanium depth profiles in the H-implanted MBE samples. For the 7 keV H-ion implantation, the H profile can be described well by a Gaussian distribution peaked at a depth of around 73 nm, approximately 120 nm above the $Si_{0.8}Ge_{0.2}$ layer. For the 33 keV H-ion implantation, the H profile appears as a

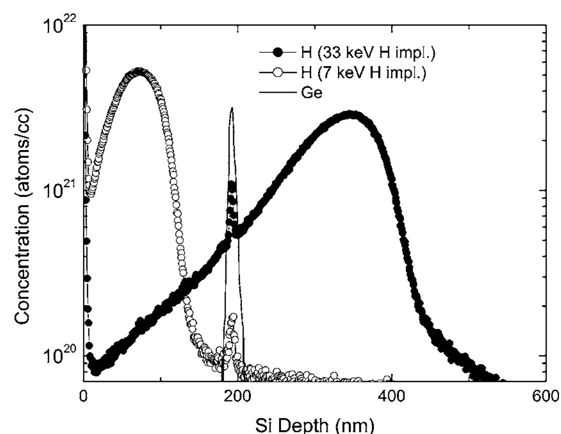

FIG. 1. SIMS depth distributions of H and Ge atoms in 7 and 33 keV H-implanted $Si/Si_{0.8}Ge_{0.2}/Si$ heterostructure containing a 5-nm-thick $Si_{0.8}Ge_{0.2}$ layer at a depth of around 200 nm.

a)Electronic mail: lshao@mailaps.org.

 © 2008 American Institute of Physics

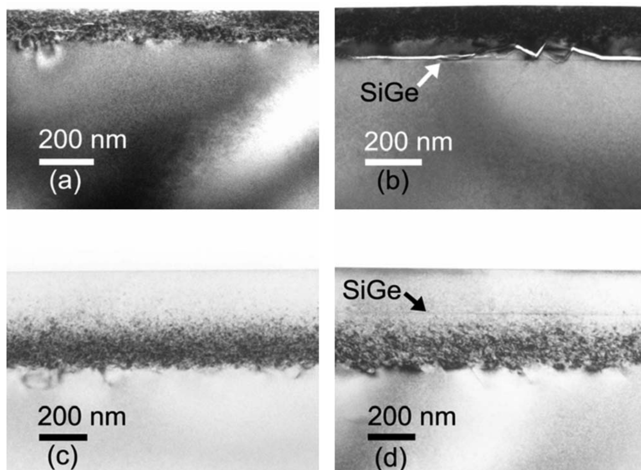

FIG. 2. TEM micrographs from H-implanted control Si (no SiGe layer) and MBE $Si/Si_{0.8}Ge_{0.2}/Si$ heterostructure. (a) 7 keV H-implanted control Si sample, (b) 7 keV H-implanted MBE sample, (c) 33 keV H-implanted control Si sample, and (d) 33 keV H-implanted MBE sample. H dosages in all implantations are $5\times10^{16}/cm^2$.

skewed Gaussian distribution. These observations agree reasonably well with transport of ions in matter (TRIM) simulations.[7] The H peak for 33 keV H-ion implantation is measured to be 342 nm, which is approximately 150 nm deeper than the $Si_{0.8}Ge_{0.2}$ layer.

Figure 1 also reveals the presence of a secondary H peak at the depth of the $Si_{0.8}Ge_{0.2}$ layer. There is no such H peak observed in the as-grown sample before H implantation (not shown). Therefore, it is concluded that the small H peak is due to H trapping by the $Si_{0.8}Ge_{0.2}$ layer. After subtracting the H background, the amount of H trapping in the $Si_{0.8}Ge_{0.2}$ layer is $5.8\times10^{13}/cm^2$ for the 7 keV H-ion implantation and $2.5\times10^{14}/cm^2$ for the 33 keV H-ion implantation. Compared with the total dose of implanted H atoms, the amount of H trapped by the $Si_{0.8}Ge_{0.2}$ layer is extremely small (less than 0.5%).

Figures 2(a)–2(d) show cross-sectional TEM micrographs from the H-implanted Si control sample and $Si/Si_{0.8}Ge_{0.2}/Si$ samples. As shown in Fig. 2(a), small (100) orientated cracks have formed in the 7 keV H-implanted Si control sample. For the strained sample after the same implantation [Fig. 2(b)], continuous cracking is observed at the depth of the $Si_{0.8}Ge_{0.2}$ layer. For the 33 keV H-ion implantation, however, there is no cracking observed at the depth of the $Si_{0.8}Ge_{0.2}$ layer [Fig. 2(d)].

The above observations suggest that (1) the $Si_{0.8}Ge_{0.2}$ layer can trap H during H-ion implantation; (2) if the H projected range is shallower than the $Si_{0.8}Ge_{0.2}$ layer, cracking occurs at the $Si_{0.8}Ge_{0.2}$ layer, even at low trapped H concentrations; and (3) if the H projected range is deeper than the $Si_{0.8}Ge_{0.2}$ layer, no cracking occurs at the $Si_{0.8}Ge_{0.2}$ layer.

We believe that H trapping is due to the interaction of hydrogen with vacancy type defects agglomerating within the $Si_{0.8}Ge_{0.2}$ layer. Previous studies have shown that vacancies prefer to cluster within the strained $Si_{1-x}Ge_x$ layer,[8,9] and H atoms have strong interactions with vacancy-type defects.[10,11] Furthermore, strain can facilitate cracking.[4,6] Our previous studies have shown that tensile strains are present within the Si adjacent to the $Si/Si_{0.8}Ge_{0.2}$ interface.[4,6] The presence of shear strains at the interface (resulting from

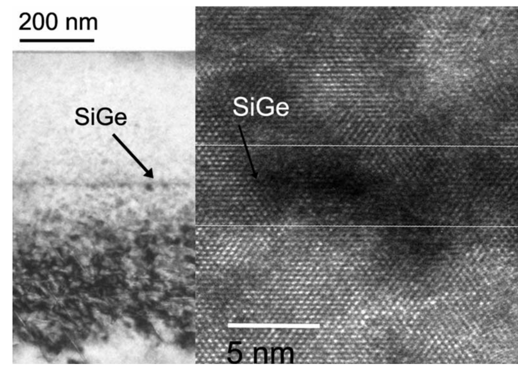

FIG. 3. TEM micrographs from 33 keV H-implanted $Si/Si_{0.8}Ge_{0.2}/Si$ heterostructure.

tensile strain in the Si and compressive strain in the SiGe) contributes a mode II component to fracture, which is in addition to the mode I component contributed by pressure inside a H platelet. For a strain layer, which is thin compared to the diameter of the platelet, the strain energy release rate for the combined strain in the strain layer and pressure inside the platelet is:[12]

$$J = \frac{(1-\nu^2)}{E}\frac{4}{\pi}(P^2a + \sigma^2 h), \tag{1}$$

where J is energy release rate, E is Young's modulus, ν is Poisson's ratio, P is the pressure inside the platelet, σ is the in-plane compressive stress in the strain layer, a is radius of the platelet, and h is the thickness of the strain layer. For brittle materials such as Si and SiGe, when the value of J exceeds the energy required to form new surfaces, a crack will propagate. Therefore, because of the presence of the strain layer, fracture will occur in smaller hydrogen platelets that will be present at lower hydrogen concentrations.

Strain plays an important role in initiating cracking. We hypothesize that significant strain relaxation occurs during 33 keV H implantation. Two mechanisms may be responsible for this. The first mechanism is ion mixing at and across the interface between Si and SiGe. Our TRIM simulation indicates that around 40% of the lattice atoms in the SiGe layer is displaced during the implantation process. This significant ion mixing can contribute to the reduction of the sharp shear strain at the interface. The second mechanism is defect-induced strain relaxation. Ion-beam-induced strain relaxation has been previously reported.[13–16] Note that the SiGe layers studied in previous reports were relatively thick. Dislocation loops were usually observed as the major defect giving rise to strain relaxation in those studies. For the ultrathin SiGe layers used in this study, we believe that point-defect clusters in the SiGe layer promote the strain relaxation.

Figure 3 shows TEM micrographs obtained from the 33 keV H-implanted MBE sample. The inset is a high resolution TEM image with the estimated position of the $Si_{0.8}Ge_{0.2}$ layer indicated by two atomic rows. Defect clusters are observed in the TEM images, adjacent to and within the SiGe layer. These defects are formed by agglomeration of ion-bombardment induced point defects.

Experimental evidence of strain relaxation in 33 keV H-implanted samples was obtained by RBS analysis. Figures 4(a) and 4(b) compare angular scans from the Ge in the strained layer before and after 7 and 33 keV H implantation, respectively. H dosages in both implantations are

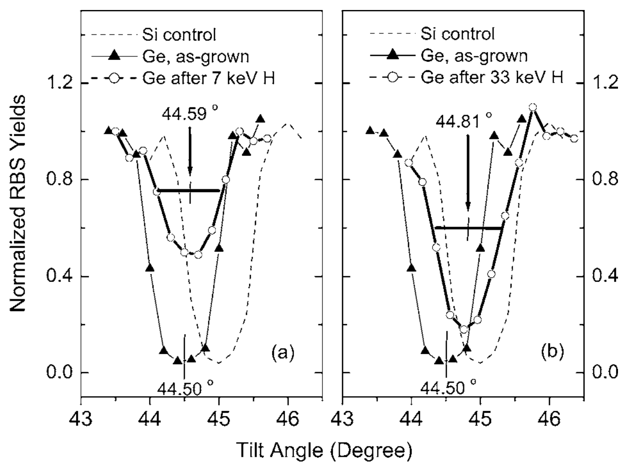

FIG. 4. Ion-backscattering yields of Ge in $Si/Si_{0.8}Ge_{0.2}/Si$ before and after (a) 7 keV and (b) 33 keV H-ion implantation, as a function of tilt angle, measured with respect to the surface normal, scanned in a (100) plane across the [110] axis. H dosages in both implantations are $3\times10^{16}/cm^2$.

3×10^{16} cm^{-2}. Scans are through the ⟨110⟩ axial direction in the (100) plane. An angular scan from the Si in a nonstrained Si substrate is also plotted for comparison. For fully strain-relaxed SiGe, the angle between the sample normal and the ⟨110⟩ axis should be 45°. For a strained SiGe layer, SiGe's in-plane lattice constant remains the same as that of Si substrate. However, stresses cause tetragonal distortion along the growth direction, resulting in a reduced angle between the sample normal and the ⟨110⟩ axis. As shown in Fig. 4(a), the midpoint of the dip in the as-grown $Si_{0.8}Ge_{0.2}$ layer is 44.50°, which is 0.50° less than 45°. This result confirms the existence of compressive strain in the layer. After 7 keV H-ion implantation, the midpoint of the angular scan dip shifts to 44.59° [Fig. 4(a)], while the midpoint of 33 keV H-implanted samples shifts to 44.81° [Fig. 4(b)].

Theoretically, the tetragonal strain in the case of pseudomorphic growth is given by

$$\varepsilon_T \equiv \varepsilon_\perp - \varepsilon_\parallel = f\frac{(1+\nu)}{(1-\nu)}, \quad (2)$$

where $\varepsilon_\perp$ is the vertical strain, $\varepsilon_\parallel$ is the in-plane strain, ν is Poisson's ratio, and f is the lattice mismatch between Si and $Si_{1-x}Ge_x$.[17] The values of ν and f are given by

$$\nu = 0.278 - 0.005x, \quad (3)$$

$$f = 0.042x, \quad (4)$$

where x is the Ge concentration.[18]

Equation (2) can be directly linked to experimental measurements through

$$\varepsilon_T = \frac{-\Delta\theta}{\sin\theta\cos\theta}, \quad (5)$$

where $\Delta\theta$ is the displacement of the ⟨110⟩ angular-scan dip from θ (45°). Substituting $\Delta\theta=-0.5$ from our as-grown strained layer in Eq. (5) gives $\varepsilon_T=0.017$, which is in good agreement with $\varepsilon_T=0.015$, the prediction from Eqs. (2)–(4) by using $x=0.2$.

These results indicate that as-grown $Si_{0.8}Ge_{0.2}$ is highly strained but strain relaxation occurs during H implantation; a comparison of the before and after ion implantation angular-scan yields shows a strain relaxation of 62% in the 33 keV H-implanted sample and a strain relaxation of 18% in the 7 keV H-implanted sample. Strain relaxation becomes significant once the strain layer is directly bombarded, when the H projected range is deeper than the strained layer.

It must be noted that H dosages in Figs. 4(a) and 4(b) for both 7 and 33 keV H implantations are 3×10^{16} cm^{-2}, which are too low to induce continuous cracking. The selection of the dosage for the RBS study is based on the fact that once cracking occurs, RBS channeling angular scan of Ge is not meaningful. We did not observe a yield dip for 5×10^{16} cm^{-2}, 7 keV H-implanted sample (due to both crack formation and extremely high dechanneling of He ions caused by shallowly located damage). As for the 5×10^{16} cm^{-2}, 33 keV H-implanted sample discussed in Fig. 2(d), a strain relaxation of 76% was measured. This strain relaxation reduces the mode II component of the strain energy release rate by 94%. These studies provide clear evidence that once significant strain relaxation occurs, the likelihood of cracking is significantly diminished.

In summary, we have shown that implanted H can be trapped by a $Si_{0.8}Ge_{0.2}$ layer buried within Si. If the H projected range is shallower than the depth of the $Si_{0.8}Ge_{0.2}$ layer, trapped H can induce continuous cracking along the $Si_{0.8}Ge_{0.2}$ layer. In contrast, if the H projected range is deeper than the depth of the $Si_{0.8}Ge_{0.2}$ layer, cracking is not observed. For such deep H-ion implantation, strain relaxation occurs as a consequence of direct ion bombardment of the $Si_{0.8}Ge_{0.2}$ layer, which reduces the strain energy release rate and makes it difficult to initiate cracking.

This research is supported by the Department of Energy, Office of Basic Energy Science, and in part by the Office of Naval Research.

[1]Q.-Y. Tong and U. Gösele, *Semiconductor Wafer Bonding* (Wiley, New York, 1999).
[2]M. Bruel, Electron. Lett. **31**, 1201 (1995).
[3]L. Shao, Y. Lin, J. G. Swadener, J. K. Lee, Q. X. Jia, Y. Q. Wang, M. Nastasi, P. E. Thompson, and N. D. Theodore, Appl. Phys. Lett. **88**, 021901 (2006).
[4]L. Shao, Y. Lin, J. K. Lee, Q. X. Jia, Y. Q. Wang, M. Nastasi, P. E. Thompson, and N. D. Theodore, Appl. Phys. Lett. **87**, 091902 (2005).
[5]P. Chen, P. K. Chu, T. Höchbauer, J. K. Lee, M. Nastasi, D. Buca, and S. Mantl, Appl. Phys. Lett. **86**, 031904 (2005).
[6]L. Shao, Y. Lin, J. G. Swadener, J. K. Lee, Q. X. Jia, Y. Q. Wang, M. Nastasi, P. E. Thompson, and N. D. Theodore, Appl. Phys. Lett. **87**, 251907 (2005).
[7]The simulation code is downloadable via http://www.srim.org.
[8]L. Fedina, O. I. Lebedev, G. Van Tendeloo, J. Van Landuyt, O. A. Mironov, and E. H. C. Parker, Phys. Rev. B **61**, 10336 (2000).
[9]A. Antonelli and J. Bernholc, Phys. Rev. B **40**, 10643 (1989).
[10]L. Shao, J. K. Lee, Y. Q. Wang, M. Nastasi, P. E. Thompson, and N. D. Theodore, J. Appl. Phys. **99**, 126105 (2006).
[11]F. A. Reboredo, M. Ferconi, and S. T. Pantelides, Phys. Rev. Lett. **82**, 4870 (1999).
[12]H. Tada, P. C. Paris, and G. R. Irwin, *The Stress Analysis of Cracks Handbook* (Del Research Corp., Hellertown, PA, 1985).
[13]B. Holländer, D. Buca, M. Mörschbächer, St. Lenk, S. Mantl, H.-J. Herzog, Th. Hackbarth, R. Loo, M. Caymax, and P. F. P. Fichtner, J. Appl. Phys. **96**, 1745 (2004).
[14]K. Sawano, A. Fukumoto, Y. Hoshi, Y. Shiraki, Y. Yamanaka, and K. Nakagawa, Appl. Phys. Lett. **90**, 202101 (2007).
[15]J. Cai, P. M. Mooney, S. H. Christiansen, H. Chen, J. O. Chu, and J. A. Ott, J. Appl. Phys. **95**, 5347 (2004).
[16]K. Kolluri, L. A. Zepeda-Ruiz, C. S. Murthy, and D. Maroudas, Appl. Phys. Lett. **88**, 021904 (2006).
[17]A. T. Fiory, J. C. Bean, L. C. Feldman, and I. K. Robinson, J. Appl. Phys. **56**, 1227 (1984).
[18]J. J. Wortman and R. A. Evans, J. Appl. Phys. **36**, 153 (1965).